SPE-190694-MS

A New Mathematical Model of Solvent - SAGD Process - Importance of Heat and Mass Transfer

Zeinab Zargar and S. M. Farouq Ali, University of Calgary

This paper was prepared for presentation at the SPE Improved Oil Recovery Conference held in Tulsa, Oklahoma, USA, 14-18 April 2018.

Abstract

The current in situ exploitation of oil sands in Alberta employs steam-based recovery methods, which are energy-intensive. A few companies are adding solvent to steam aiming to reduce steam requirements. The mechanism of oil recovery by steam with added solvent is not clear. Over the years, on several occasions- as at the present time- the oil industry has resorted to the use of solvents with steam in thermal recovery operations. The past trials with solvent were short-lived in view of the cost of solvents as well as the lack of success. Given the controversy regarding the use of solvents with steam, this work is intended to explain whether solvent injection with steam increases oil recovery or not.

In this work, a new analytical model is developed for describing the solvent-SAGD performance based on the combination of an overall solvent mass balance, heat balance and volumetric oil displacement and Darcy's oil rate using a mixture viscosity model as a function of temperature and solvent concentration ahead of front which satisfy the equilibrium in the system.

The objectives of this work are to predict: vapour-steam chamber growth, oil production rate, solvent production rate, solvent loss (or solvent retention) rate, and the effect of solvent type and concentration on the solvent-SAGD process. The results show that the rate of solvent retention increases over time, while the production rates of solvent and bitumen decrease.

The efficiency of this process is evaluated using Cumulative Steam-Oil Ratio (CSOR) and cumulative solvent-oil ratio, which permits a comparison of the efficiency of SAGD and solvent-SAGD processes for different solvents. On the whole, the results of this approach give a better understanding of the mechanism of oil production during the solvent-SAGD process by interconnecting vapour chamber conditions and the conditions of heated and diluted oil ahead of the interface.

Introduction

There are some limitations in applying Steam Assisted Gravity Drainage (SAGD) for oil sands, such as high steam requirement with steam generation resulting in significant greenhouse gas emissions. The oil industry has resorted to developing new processes to overcome this shortcoming. Adding a small amount of condensable gas as a solvent to steam was proposed as one of the solutions, named variously as Expanding Solvent Steam-Assisted Gravity Drainage (ES-SAGD), Solvent Aided Process (SAP), or Liquid Addition

to Steam for Enhanced Recovery (LASER), etc. The economics of these processes depends on the oil production rate, solvent requirement and solvent retention in view of the high cost of solvents. In addition, it remains unclear which solvent results in better recovery, if any, compared to the steam only process, and what would be the optimal amount of solvent concentration in the injected steam. Evaluating the performance of this process has mostly been done by numerical simulation. There are only a few analytical treatments of this process.

Past Studies

Extensive work was done on solvent-steam processes back in 1960-70's by Farouq Ali, Allen and Redford and others. Butler and Mokrys (1989) proposed a mathematical model of the VAPEX (Vapour Extraction) process analog of SAGD. In this process solvent as a vapour replaces the steam chamber in SAGD but at considerably lower temperatures. VAPEX is not a thermal method, the main recovery mechanism is mass transfer instead of heat transfer unlike SAGD, which is several orders of magnitude slower that heat transfer. The process had limited success in the field. Experimental studies were performed by Das and Butler (1998) to evaluate VAPEX. Results show that the performance of VAPEX is considerably improved by using vaporized solvent than liquid due to the higher gravity force and lower solvent retention. It was observed that the maximum oil recovery was achieved with propane or butane. Coinjection of small amount of solvent, mostly light to medium hydrocarbons, with steam has been investigated as an alternative to heavy oil recovery method to improve the efficiency of steam only (SAGD) or solvent only (VAPEX) gravity driange processes by combining them. Nasr and Isaacs (2001) introduced the Expanding-Solvent Steam-Assisted Gravity Drainage (ES-SAGD) process. The process was tested in field scale, and it showed better thermal efficiency, lower water requirement and in some cases better oil recovery compared to SAGD. It was suggested that the solvent should condense or evaporate at conditions similar to that for water at the operating pressure. Gupta and Gittins (2011) developed a semi-analytical model for estimating oil rate by combining SAGD and VAPEX equations.

The model is concerned with the amount of solvent dissolution in oil, and solvent concentration in the vapour phase at the front. It was suggested that by assuming an artificially increased molecular diffusion coefficient (by almost two order of magnitude) or by introducing a diffusive solvent layer in between the vapour chamber and the oil zone, the oil production rate from the model could be justified. The model predicted that butane and pentane result in higher oil rates compared to hexane. Azom (2013) developed a model for estimating dimensionless and time independent drainage rate as a function of thermo capillary number by considering multiphase flow, showing that below a certain range of thermo-capillary number (which is mostly at field scale) ES-SAGD does not show improvement over SAGD. Rabiei et al. (2014) extended Butler's SAGD model (1985) to include the effect of mass transfer in addition to heat transfer. The heat integral method was applied to solve the unsteady state temperature and concentration profiles.

Premises of the Present Model

In this work, by assuming a constant rate of steam and solvent injection and relating this to the vapour chamber and the mobilized oil ahead of the vapour and oil interface, an analytical model is derived for evaluating the solvent-SAGD process. In this study, unlike previous models, it is assumed that the injected solvent vapour condenses at the chamber edges and the heat and mass fluxes at the vapour chamber interface are the limiting boundary conditions. The injected solvent travels with steam in different directions; there would be the accumulation of solvent around the boundaries of the chamber. The accumulated solvent at the edges of the vapour chamber condenses to keep the vapour chamber at the concentration of the injected solvent. At the advancing front, the condensed solvent mixes with the oil and reduces oil viscosity. The solvent accumulated at the top boundary of the reservoir is assumed to be retained inside the vapour chamber. A conservative solvent loss model is assumed in this approach which is similar to the conservative heat loss term in the energy balance equation.

Model Development

Zargar and Farouq Ali (2017) proposed a Constant Heat Injection (CHI) model for the SAGD process, based on a constant steam (heat) injection rate. It was shown that due to the increasing heat loss and interface extension, oil rate decreased over time. This approach is extended in this work to include solvent co-injection with steam at a constant total rate of injection.

The vapour chamber shape is represented by an inverted triangle fixed at the producer. The model is developed for an arbitrary interface at $t = t_n$ and position $\theta = \theta_n$. The horizontal vapour chamber velocity at the top of the reservoir (x'_H) is the primary unknown in the equations. This maximum horizontal vapour chamber velocity is obtained from a combination of an overall solvent mass balance, heat balance and volumetric oil displacement and Darcy's oil rate using a mixture viscosity model as a function of temperature and solvent concentration ahead of the front which satisfies equilibrium in the system. It is assumed that mass and heat diffusion occur in a direction normal to the interface.

Temperature and Concentration Profiles

It is assumed that the total injection rate (solvent and steam) is constant. The temperature and concentration differential equations are developed, for a linear vapour chamber interface and an arbitrary interface at $t = t_n$ and position $\theta = \theta_n$.

Overall Heat Balance

In this approach, heat loss to the overburden and constant injection rate are expected to have a limiting effect on the growth rate of the chamber. Based on the overall heat balance, constant heat injected at a constant rate is distributed in the reservoir in three different ways: heat loss rate to the overburden, rising vapour chamber and the produced oil temperature increase from T_r to T_s, and outflow of heat into the oil zone ahead of the advancing front, assumed to be by conduction only. In the solvent SAGD process, the injected heat is the sum of the latent heats of vaporization of steam and solvent.

$$q_{inj} = i_{tot}\left\{\left(1 - C_{sol}^{inj}\right)f_s^{st}L_v^{st} + C_{sol}^{inj}f_s^{sol}L_v^{sol}\right\} \tag{1}$$

In the above equation i_{tot}, is the total mass rate for solvent and steam and C_{sol}^{inj} is the injected mass fraction of solvent.

From the above equation, it can be concluded that heat injection rate in case of solvent-SAGD is smaller than in SAGD due to the presence of the solvent in the vapour and, in turn, the considerable lower latent heat of vaporization of the solvent.

Overall heat balance can be written as:

$$q_{res} = q_{inj} - (q_{loss} + q_{sc}) \tag{2}$$

Heat loss rate in a conservative design can be calculated as:

$$q_{loss} = \frac{2\,K_{ob}\Delta T}{\sqrt{\pi\alpha_{ob}}}\frac{x_H}{\sqrt{t}} \tag{3}$$

And heat rate for vapour zone expansion is evaluated as

$$q_{sc} = \frac{\partial}{\partial t}(MC(T_s - T_r)) = Hx'_H(\rho C)_{res}\Delta T \tag{4}$$

The portion of injected heat which flows into the oil zone at a rate q_{res} at the vapour chamber interface is given by:

$$q_{res} = -K_{res}A_{inf}\left(\frac{dT}{d\xi}\right)_{\xi=0} \tag{5}$$

Hence, by substituting Equations (3), (4) and (5) into the energy balance equation, the temperature gradient at the interface is given by:

$$\left(\frac{dT}{d\xi}\right)_{\xi=0} = -\frac{sin\theta}{2K_{res}H}\left\{q_{inj} - \left(\frac{2K_{ob}\Delta T}{\sqrt{\pi\alpha_{ob}}}\frac{x_H}{\sqrt{t}} + Hx'_H(\rho C)_{res}\Delta T\right)\right\} \tag{6}$$

Diffusive Frontal Velocity

Figure 1 shows that the front is moving with a constant velocity U (normal to vapour chamber interface) for each interface position. The relation between U and x'_H is

$$U = x'_H\, sin\theta_n \qquad where\ \theta_n = \tan^{-1}\left(\frac{H}{x_n}\right) \tag{7}$$

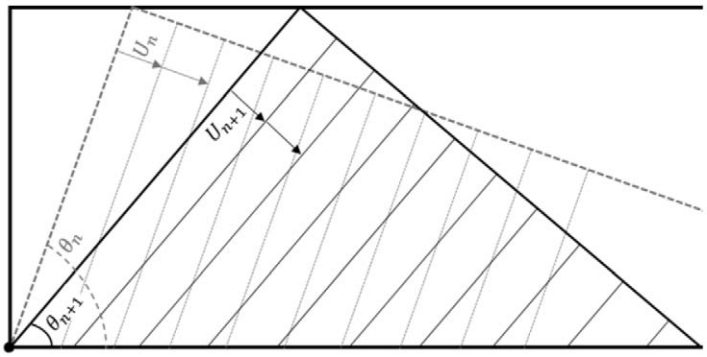

Figure 1—Front movement for each steam chamber interface.

Given that the volume displacement in the front movement should be equivalent to vapour chamber interface movement, the front velocity is modified to correctly represent the vapour chamber interface movement. From Figure 2, triangle ABD has the same area as the parallelogram ABCF. So,

$$U_f = \frac{1}{2}x'_H\, sin\theta_n \tag{8}$$

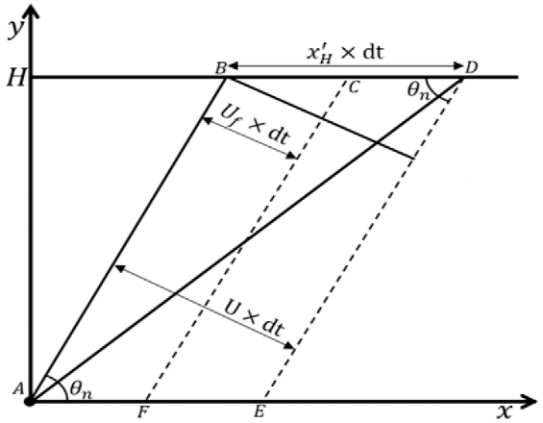

Figure 2—Steam chamber movement should be equal to front movement.

Equation (8)) indicates that the front velocity depends on the vapour chamber interface positions and unknown chamber velocity.

Temperature Equation

Heat is assumed to be transferred ahead of the interface by conduction only, expressed by:

$$\frac{\partial^2 T}{\partial Z^2} = \frac{1}{\alpha}\frac{\partial T}{\partial t} \tag{9}$$

The vapour chamber expansion is a moving boundary problem. Pseudo steady-state temperature equation and the two boundary conditions ahead of a moving front (ξ coordinate) at $t = t_n$ are given by:

$$\begin{aligned} &\frac{d^2T}{d\xi^2} + \frac{U_f}{\alpha}\frac{dT}{d\xi} = 0 \\ &\left(\frac{dT}{d\xi}\right)_{\xi=0} = -\frac{sin\theta}{2K_{res}H}\left\{q_{inj} - \left(\frac{2K_{ob}\Delta T}{\sqrt{\pi\alpha_{ob}}}\frac{x_H}{\sqrt{t}} + Hx'_H(\rho C)_{res}\Delta T\right)\right\} \\ &T(\xi \to \infty) = T_r \end{aligned} \tag{10}$$

Therefore, by solving the above equation, the temperature profile at each given time or interface position can be calculated as:

$$T(\xi, t) = \frac{\alpha}{K_{res}Hx'_H}\left\{q_{inj} - \left(\frac{2K_{ob}\Delta T}{\sqrt{\pi\alpha_{ob}}}\frac{x_H}{\sqrt{t}} + Hx'_H(\rho C)_{res}\Delta T\right)\right\} e^{-\frac{sin\theta}{2\alpha}x'_H\xi} + T_r \tag{11}$$

Note that over time, the temperature profile from this model is affected by gravity, variation of maximum vapour chamber velocity (at the top), heat injection rate, etc.

Overall Solvent Mass Balance

The injected solvent into the process can be consumed in three ways: accumulation as a vapour phase in the growing vapour chamber, diffusion into the oil zone, and retention in the system. It is assumed that the solvent concentration in the vapour chamber is equal to the injection point concentration. The overall mass balance for solvent can be written as:

$$\dot{m}|_{in} - \dot{m}|_{out} = \frac{\partial M_{sol}}{\partial t} \tag{12}$$

$$\dot{m}|_{in} = C_{sol}^{inj} i_{tot} \tag{13}$$

Where $\dot{m}$ and M_{soi} are mass flow rate and mass accumulation within the system. The injected solvent as a vapour phase travels with steam in all directions. As a result, it accumulates at the boundaries of the vapour chamber condensing as it reaches the required concentration and temperature for phase change. In our model, there are two boundaries; overburden rock at the top and vapour-oil interface. Both of these boundaries extend over the course of time. As a result, the vapour loses heat at the boundaries. Steam provides heat to the system, and solvent diffuses into the oil zone and dilutes the bitumen, the main goal is a combination of these two mechanisms which reduces the bitumen viscosity and supports enhanced recovery and net energy efficiency. The solvent plays a role in reducing oil viscosity if it condenses at the vapour-oil interface. Thus, solvent condensation at any other place is considered to be a loss.

$$\dot{m}|_{out} = \dot{m}|^{top} + \dot{m}|^{front} \tag{14}$$

Condensed solvent at top and the front can be related as: $ri|^{top}\ x_H$

$$\frac{\dot{m}|^{top}}{\dot{m}|^{front}} = \frac{x_H}{L_{int}} \tag{15}$$

$$\dot{m}|^{top} = \cos\theta_n \, \dot{m}|^{front} \tag{16}$$

$$\dot{m}|_{out} = (1 + \cos\theta_n) \, \dot{m}|^{front} \tag{17}$$

We call it conservative design for the solvent loss. The above equation indicates that at the beginning of the process starting ($\theta_n = \frac{\pi}{2}$), there is no solvent mass loss and all the injected solvent diffuses into the oil zone and stored in the growing chamber as vapour. Over time, due to increasing solvent loss (retention), mass flux at the front decreases.

$$\frac{1}{2} C_{sol}^{inj} i_{tot} - (1 + \cos\theta_n) \, \dot{m}|^{front} = \frac{1}{2} H\phi S_v \rho_{sol}^{v} x'_H \tag{18}$$

$$S_v = 1 - S_{or} \tag{19}$$

C_{sol}^{inj} is the injected solvent mass fraction, and S_v is the saturation of the vapour phase in the depleted chamber.

It is assumed that all the condensed solvent at the vapour-oil interface is available to diffuse into the oil zone and contributes to bitumen dilution. The rate of mass diffusion can be calculated based on Fick's law in the direction normal to the interface as:

$$\dot{m}|^{front} = -D_{so} A_{int} \rho_{sol} \left(\frac{\partial C}{\partial \xi}\right)_{\xi=0} \tag{20}$$

For a unit length of the horizontal well,

$$A_{int} = 1 \times L_{int} = \frac{H}{\sin\theta_n} \tag{21}$$

In the above equation, C is the volume fraction of solvent in the fluid mixture, D_{so} is the diffusivity coefficient of the solvent into the bitumen. Substituting the above equations into the solvent mass balance equation,

$$\frac{1}{2} C_{sol}^{inj} i_{tot} + (\csc\theta_n + \cot\theta_n) D_{so} \rho_{sol} H \left(\frac{\partial C}{\partial \xi}\right)_{\xi=0} = \frac{1}{2} H\phi (1 - S_{or}) \rho_{sol}^{v} x'_H \tag{22}$$

There are two unknowns in the above equation; concentration gradient at the interface, $\left(\frac{\partial C}{\partial \xi}\right)_{\xi=0}$, and vapour chamber velocity, x'_H. The concentration gradient can be obtained based on the vapour chamber velocity as:

$$\left(\frac{\partial C}{\partial \xi}\right)_{\xi=0} = -\frac{0.5}{(\csc\theta_n + \cot\theta_n) D_{so} \rho_{sol} H} \left\{ C_{sol}^{inj} i_{tot} - H\phi (1 - S_{or}) \rho_{sol}^{v} x'_H \right\} \tag{23}$$

So, the concentration gradient at the interface is a function of solvent concentration at the injection point, total injection rate, interface angle, reservoir rock and fluid properties and most importantly the vapour chamber velocity. This concentration gradient at the interface will be used as a Neumann boundary condition for the concentration equation in differential form.

One-dimensional advection-diffusion equation in a direction normal to the vapour chamber interface without bulk flow in this direction and assuming a constant diffusion coefficient can be written as:

$$\frac{\partial C}{\partial t} = D_{so}\frac{\partial^2 C}{\partial Z^2} \tag{24}$$

For a diffusive front velocity U_f, the pseudo-steady state concentration equation and the boundary conditions are given by:

$$\frac{d^2C}{d\xi^2} + \frac{U_f}{D_{so}}\frac{dC}{d\xi} = 0$$
$$\left(\frac{\partial C}{\partial \xi}\right)_{\xi=0} = -\frac{0.5}{(\csc\theta_n + \cot\theta_n)D_{os}\rho_{sol}H}\left\{C_{sol}^{inj} i_{tot} - H\phi(1-S_{or})\rho_{sol}^{v} x'_H\right\} \tag{25}$$
$$C(\xi \to \infty) = 0$$

Solving this equation, the concentration distribution ahead of the advancing front is given by:

$$C(\xi,t) = \frac{1}{(1+\cos\theta)\rho_{sol}x'_H}\left\{\frac{i_{tot}C_{sol}^{inj}}{H} - \phi(1-S_{or})\rho_{sol}^{v}x'_H\right\} e^{-\frac{1}{2D_{so}}sin\theta x'_H\xi} \tag{26}$$

Knowing the temperature and concentration profiles ahead of advancing front, the reduced bitumen viscosity can be predicted under the effect of heating and dilution.

Viscosity Model

In the solvent-SAGD process, bitumen drainage rate mainly depends on viscosity reduction by heat and solvent mass transfer, apart from gravity as the main driving force. Bitumen viscosity should be determined based on the temperature and concentration distributions ahead of the advancing front. In this study, a mixture viscosity (solvent and bitumen) model as a function of temperature is developed from the combination of Andrade's viscosity-temperature equation (1932)) and Shu's mixture viscosity equation (1984)).

Andrade's viscosity model as a function of temperature is given by:

$$\mu = ae^{\frac{b}{T}}, \tag{27}$$

where a and b are constants and μ is viscosity in centipoise which are evaluated for bitumen, butane, pentane and hexane using bitumen and solvent viscosities data given by Gupta and Gittins (2011) and shown in Table 1.

Table 1—Andrade's constants used in this study.

	Bitumen	Butane	Pentane	Hexane
a	1.355E-4	2.54E-3	4.3717E-3	0.01772
b	5318.123	1239.98	1184.6	834.89

Figure 3 shows the results of the mixture viscosity model used in this study. The figure indicates that the mixture viscosity is always lower than bitumen viscosity over the entire range of temperature. It also can be seen that the higher the solvent concentration, the lower the mixture viscosity. The other point that can be concluded from Figure 3 is that the solvent effect on bitumen viscosity reduction is more significant at lower temperatures compared with higher tempertures.

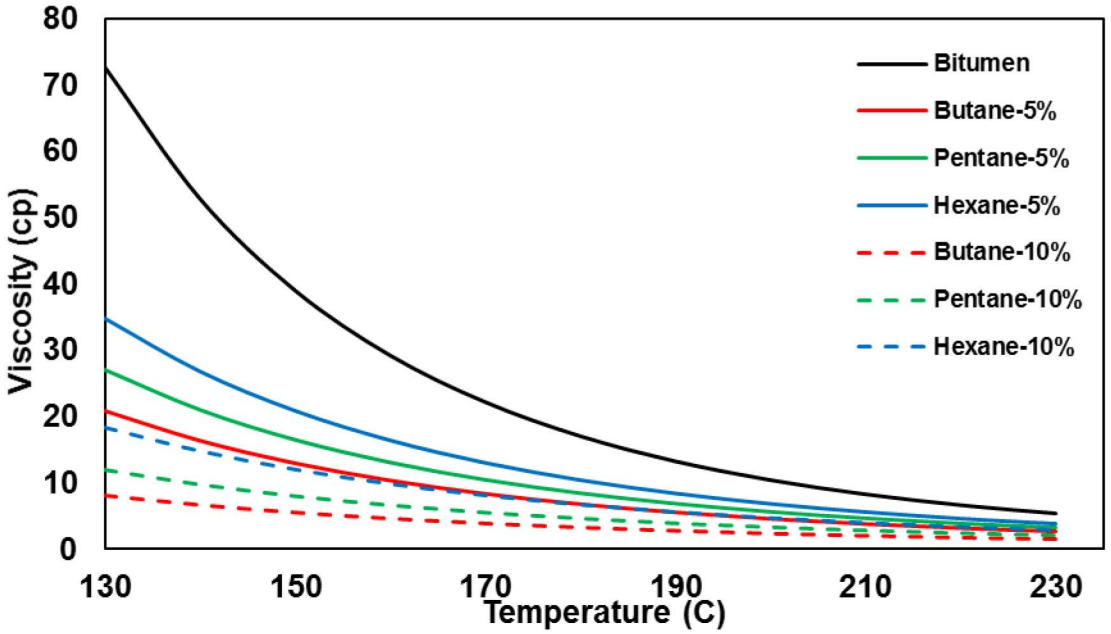

Figure 3—Mixture viscosity model as a function of temperature for vaious solvents; butane, pentane, and hexane and different solvent volume fractions with bitumen; 5 and 10%.

Oil Drainage

Volumetric oil displacement as a result of vapour chamber interface movement (x'_H), assuming an inverted triangle approximation for the steam chamber growth is calculated as:

$$q_o = \frac{1}{2} H \phi \Delta S_o x'_H \tag{28}$$

Another equation for calculating oil drainage rate is from Darcy's law. Heated and diluted bitumen flows down to the production well in the direction parallel to the vapour-oil interface the gravity force being the primary drive. Thus, the oil flow rate for a small element parallel to the vapour chamber interface is given by:

$$dq_o = \frac{k_o \, \rho_o g \, sin\theta_n}{\mu_o} d\xi \tag{29}$$

Ahead of a particular vapour-oil interface at a given moment, bitumen viscosity varies significantly in the direction normal to the interface which is the main reason for oil mobility in this zone. It is assumed that the oil density variation with temperature, is negligible compared to the viscosity change. The oil rate as a function of temperature and concentration, and in turn distance from the interface, in the direction normal to the interface results, for this particular interface position is given by:

$$q_o = k_o \, \rho_o g \, sin\theta_n \int_0^\infty \frac{1}{\mu_o(\xi)} d\xi \tag{30}$$

The viscosity model introduced in the previous section is used to calculate the integral. The primary unknown in this set of equations (11), (26), (28), and (30) is the vapour chamber velocity. Because of the non-linearity of the model equations, an iterative method is used to find the vapour chamber velocity (x'_H) which satisfies these equations. By predicting the vapour chamber velocity, oil production rate, heat distribution in the system, rate of solvent retention, solvent production rate, and the efficiency of the solvent SAGD process can be compared to the SAGD process at the same total mass of injection.

Results

Figure 4 compares oil production rate of SAGD and solvent-SAGD for butane, pentane, and hexane (at the same mass fraction 9%) by use of data given in Table 2. As it can be seen adding solvent, increases oil production rate in case of using butane but decreases by injecting pentane and hexane. The figure shows that the heavier the solvent, the lower oil production rate is achieved. Bitumen production rate is almost the same in case of injecting pentane with steam and steam only. But, it should be noted that in Figure 5, it is shown that CSOR in case of injecting pentane is lower.

CSOR does decrease when the solvent is injected with steam. The results are shown in Figure 5. In the best case of butane, CSOR for a 9% slug is 1.92 which is nearly 17% reduction compared with the no solvent case of 2.32 (m^3/m^3).

Figure 6 shows the total hydrocarbon (solvent plus bitumen) production rate over a 1000-day time interval. The curves of solvent and bitumen production rate start with much higher initial rates and then decrease sharply compared with SAGD oil production rate.

CSOR versus cumulative oil production for different solvents are compared in Figure 7. It can be concluded from the curves that at the same cumulative oil production, highest CSOR is for SAGD and the lowest one is for the butane 9%-SAGD.

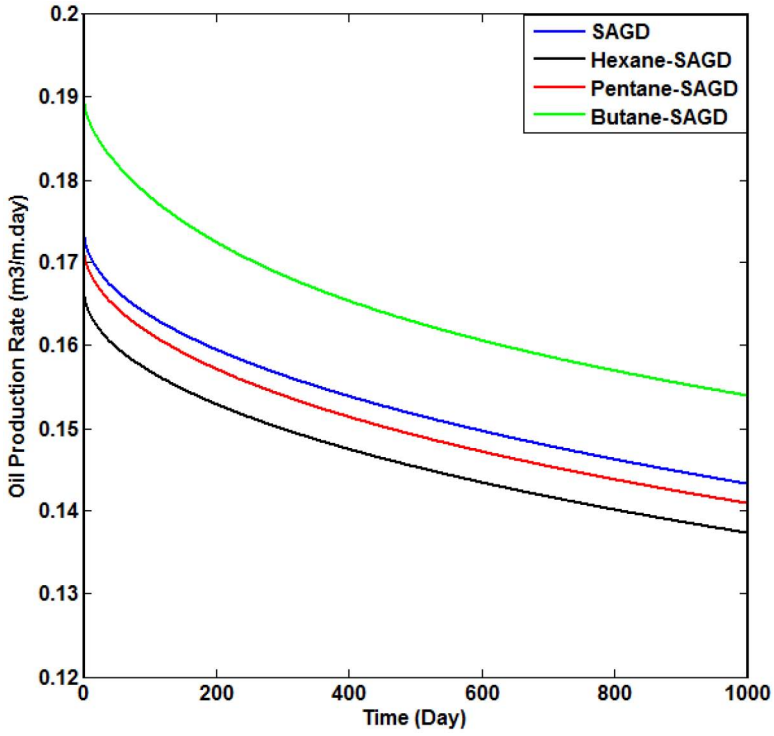

Figure 4—Comparison of oil production rate from solvent 9%-SAGD with SAGD.

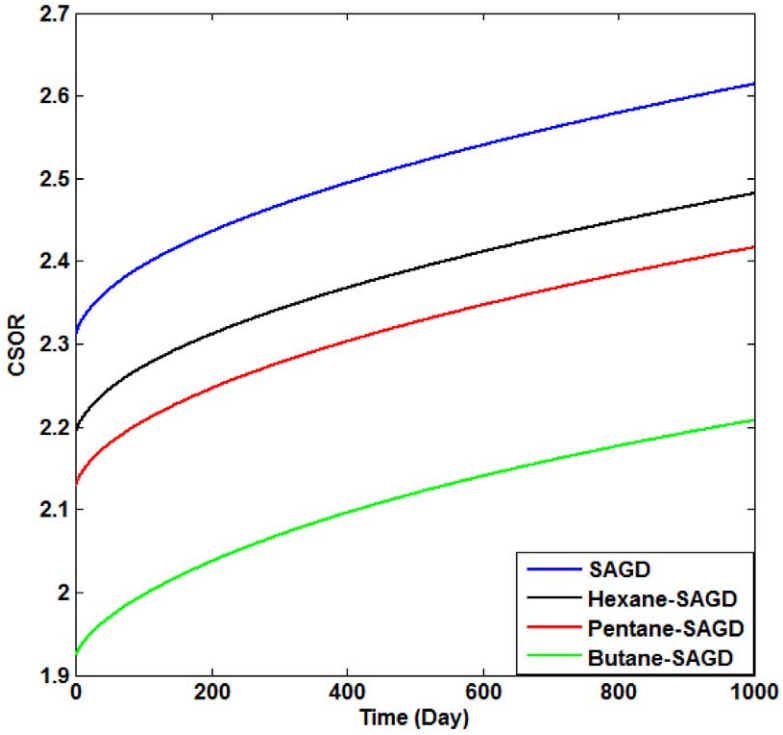

Figure 5—Comparison of CSOR of solvent 9%-SAGD with SAGD.

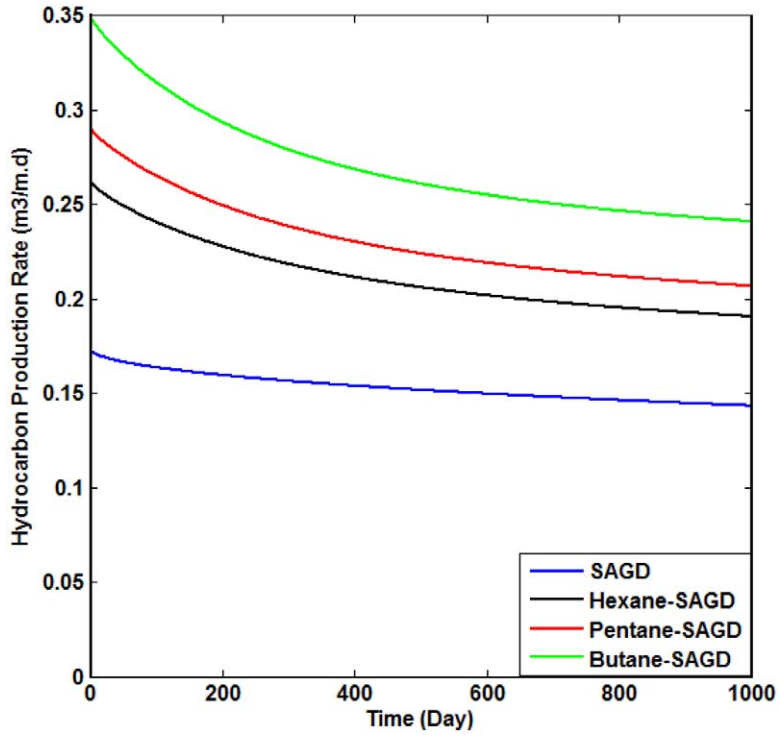

Figure 6—Solvent and bitumen production rate over a 1000-day period for different solvent at the same mass fraction (9%).

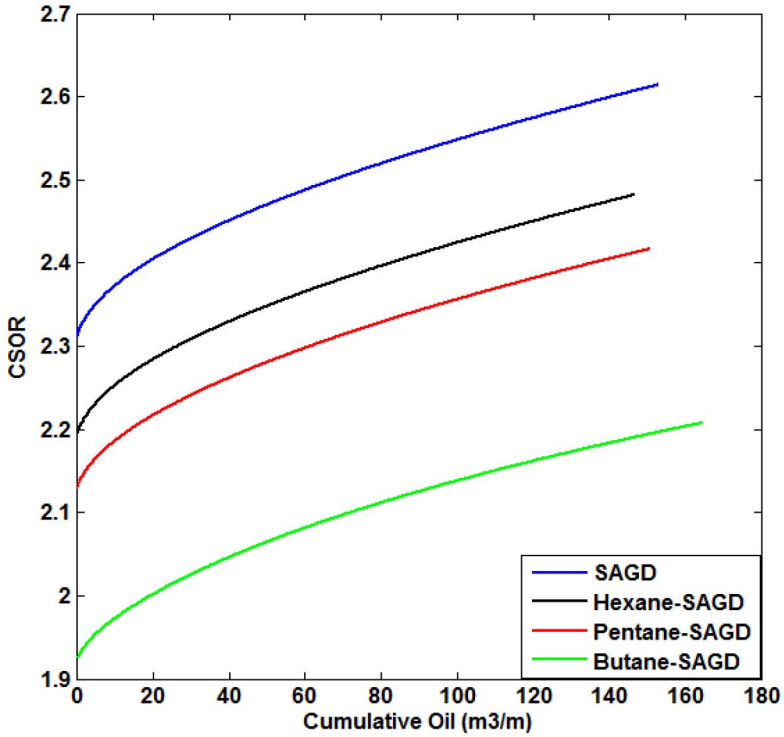

Figure 7—Comparison of cumulative steam-oil ratio versus cumulative bitumen production for different solvent co-injection (at the same mass fraction 9%) with steam and steam only.

Effect of two slug sizes 5%, and 9% is investigated on the performance of the solvent-SAGD process in Figures 8, 9, and 10.

Figure 8 shows the oil production rate as a function of time. A higher oil rate is achieved in the case of butane (about 12% increase) and a higher mass fraction of butane, 9% compared with 5%, results in a higher oil rate. When heavier hydrocarbons such as pentane and hexane are employed, the figure shows that oil rate is lower compared with steam only. As can be seen, in the cases of inj ecting pentane or hexane with larger mass fraction of 9%, a lower oil production is resulted in comparison to mass fraction of 5%. This behaviour is opposite to the case of butane as solvent.

Hydrocarbon production rate for two different mass fractions, 5 and 9%, are compared in Figure 9. The larger mass fraction results in higher hydrocarbon (solvent and bitumen) production rate. Solvent production is greater in the case of larger solvent slug in addition to the mixed behaviour of oil production rate in all cases (butane, pentane, and hexane). These effects are summarized in Table 3.

Figure 10 compares CSOR for different solvents with different mass fraction. CSOR is defined as cumulative steam injected to cumulative bitumen production. In the case of larger mass fraction, the cumulative steam injected is lower, and but cumulative oil production can be higher or lower depending on solvent type compared with the smaller one. The combination of these two effects results in lower CSOR in the case of larger mass fraction as it can be seen in Figure 10.

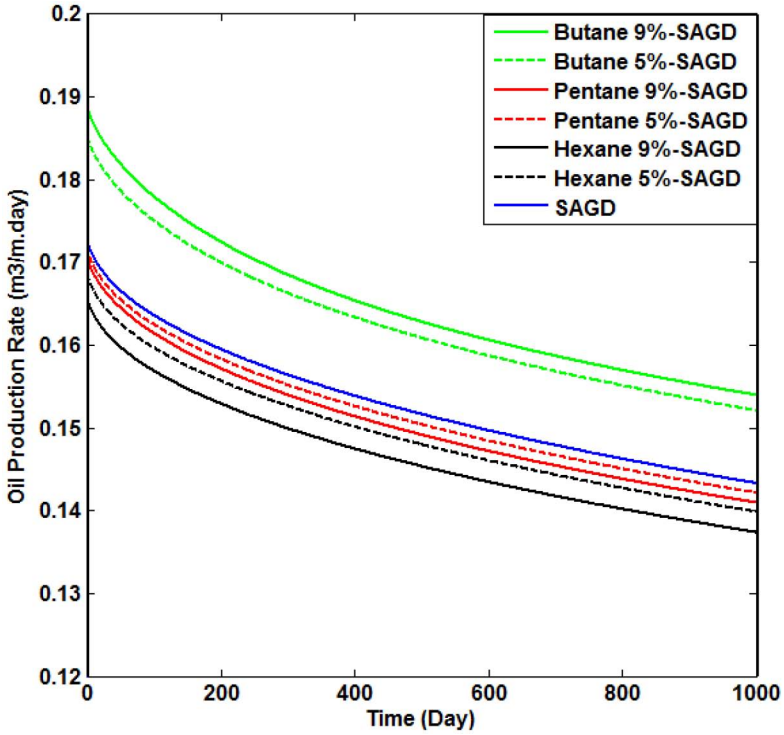

Figure 8—Effect of solvent mass fraction on oil production rate for various solvents.

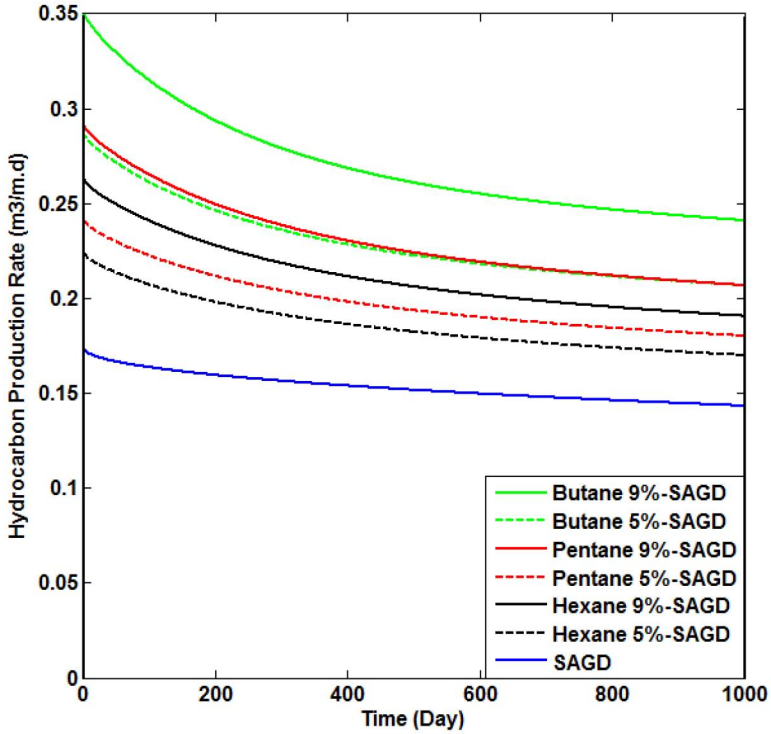

Figure 9—Effect of solvent mass fractionon total solvent and bitumen production rate for various solvents.

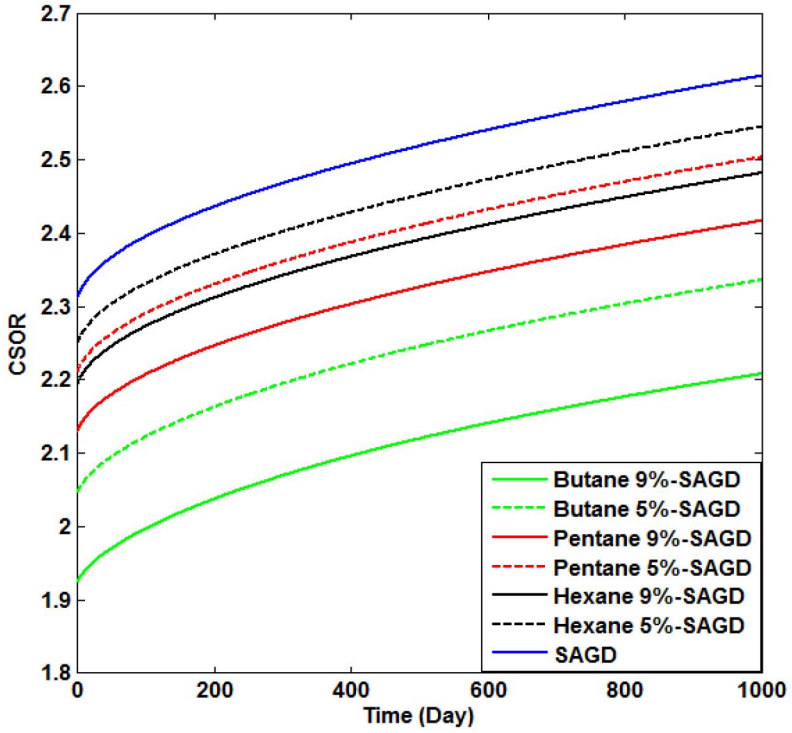

Figure 10—Cumulative steam oil ratio over a 1000-day period for different solvents and different solvent mass fraction (5 and 9%).

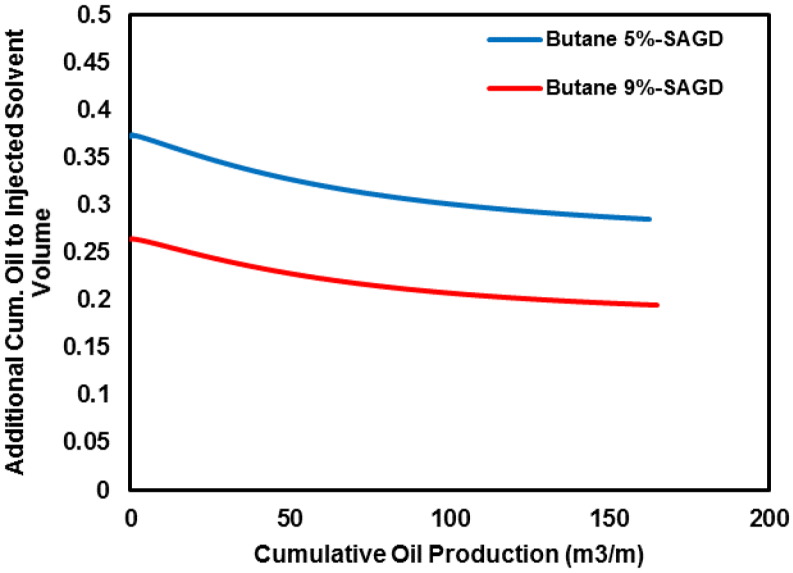

Figure 11—Comparison of additional cumulative oil to cumulative injected solvent number versus cumulative oil production for butane at two different mass fractions of 5 and 9%.

Figure 11 compares the *additional* cumulative oil to injected solvent number for butane for mass fraction of 5 and 9%. These curves show that the additional cumulative oil to injected solvent number is positive in case of butane-SAGD process. This indicates that the oil recovery increases in case of replacing some of steam in SAGD process with butane. However, the number is low (much lower than 1) which indicates that the gain in bitumen production is lower than the injected butane volume. The larger the mass fraction of butane (9%) results in lower numbers.

Table 3 summarizes the results of the solvent-SAGD model for various solvents (butane, pentane, and hexane) and different mass fractions (5 and 9%), at the same total mass of injection (400 kg/day-m), using the reservoir properties shown in Table 2 which can be explained as follows:

Additional oil-to-solvent volume ratio

An important number in the solvent-steam injection is the ratio of the additional cumulative oil produced to the injected solvent volume. Additional oil is defined as the oil produced minus the oil produced in the no-solvent case. If this ratio is 1.0, then it means that the gain in bitumen production is same as the volume of solvent injected. This number is seen to be much smaller than 1.0 and is 0.29 and 0.2 in the best case of butane 5% and 9% respectively. In case of pentane and hexane is even negative, indicating that the solvent reduced oil recovery.

Effect of solvent on oil recovery

Cumulative oil production increases when butane is used as a solvent, compared to no solvent. For a 5% slug, the cumulative oil is highest for butane (162.7 vs. 153 m^3 for no solvent). For a 9% slug, the cumulative oil recovery is again highest for butane (165 vs. 153 m^3 for no solvent). This behaviour is opposite for the other solvents; lower cumulative oil production and larger the solvent mass fraction lower is the cumulative oil production.

Solvent production and loss

As expected from the model, solvent production rate decreases over time while solvent loss rate increases. This can be seen from the results shown in the table. Solvent loss and production increases as the mass fraction increases from 5 to 9%.

Cumulative solvent-oil ratio

The lower the cumulative solvent-oil ratio, the better is the efficiency of the solvent-SAGD process. From Table 3, the larger the mass fraction regardless of solvent type, the higher is this ratio. The results also indicate that the heavier hydrocarbons are more desirable in view of the solvent efficiency.

Heat injection rate

Table 3 shows that the highest heat injection rate apart from SAGD (6.84E+05 kJ/d.m) is in the case of butane 5% (6.81E+05 kJ/day.m), indicating only a small difference. This is because of the higher latent heat of vaporization of water at the lower saturated temperature or pressure. The heat injection rate decreases from the lighter to the heavier solvents.

Of the 1530 SAGD well pairs in operation (total is about 1800), about 50 are using solvent in some forms (e.g. initial communication between the wells instead of heating, injection with steam as slugs, injection late in a mature project, etc.). The available field results show an increase in bitumen production in some cases, and no gain in others. Often the increase is not defined, i.e. the bitumen volume produced also includes solvent produced. This was observed in the present model results also, viz. the total hydrocarbon (bitumen plus solvent) volume produced increased when a solvent was injected with steam. However, the net gain in bitumen produced (compared to plain SAGD) was invariably smaller than the injected solvent volume.

Table 2—Rock and fluid properties used in this study.

Porosity	0.35
Reservoir height, m	22
Oil density at reservoir temperature, kg/m^3	1014
Rock density, kg/m^3	2040
Overburden rock density, kg/m^3	2400
Molecular weight of oil, g/mol	500
Specific heat capacity of oil, J/(kg.°C)	2093
Specific heat capacity of overburden rock, J/(kg.°C)	837
Specific heat capacity of reservoir rock, J/(kg.°C)	936
Initial reservoir temperature, °C	6
Gas constant, J/(K.mole)	8.314
Reservoir rock thermal conductivity, J/(s.m.°C)	1.3
Overburden thermal conductivity, J/(s.m.°C)	1.73
Initial oil saturation	0.75
Residual oil saturation	0.14
Accelaration of gravity, m/s²	9.8
Effective Permmeability, m^2	0.8×10^-12

Table 3—Results of the solvent-SAGD model for different solvents and mass fraction over a 1000-day time interval (day 1 to day 1000).

Injected Solvent	NONE	C4H10	C4H10	C5H12	C5H12	C6H14	C6H14
Injected solvent concentration, w%	0	0.05	0.09	0.05	0.09	0.05	0.09
Solvent molecular weight (g/mol)		58.12	58.12	72.15	72.15	86.18	86.18
Solvent density at reservoir temperature, kg/m^3		591	591	632	632	666	666
Total injection rate (Steam and Solvent), kg/day-m	400	400	400	400	400	400	400
Chamber temperature, °C	232.5	214	205	226	221	229	225.5
Latent heat of vaporization of steam, J/kg	1800000	1881000	1915000	1830000	1853000	1817000	1834000
Steam pressure, MPa	2.94	2.075	1.75	2.6	2.36	2.75	2.55
Oil production rate, m^3/day-m	0.1730 to 0.1433	0.1856 to 0.1521	0.1891 to 0.1539	0.1719 to 0.1421	0.1709 to 0.1409	0.1688 to 0.1398	0.1659 to 0.1374
Solvent production rate, m^3/day-m	-	0.1007 to 0.0547	0.1605 to 0.0870	0.0693 to 0.0380	0.1199 to 0.0658	0.0548 to 0.03	0.0966 to 0.0533
Solvent loss rate, m^3/day-m	-	0 to 0.0462	0 to 0.0737	0 to 0.0314	0 to 0.0543	0 to 0.0248	0 to 0.0436
CSOR, m^3/m^3	2.3 to 2.62	2.05 to 2.34	1.925 to 2.208	2.2 to 2.5	2.13 to 2.42	2.25 to 2.545	2.19 to 2.48
Cumulative Solvent Oil Ratio, m^3/m^3	-	0.546 to 0.623	0.8538 to 0.9793	0.4065 to 0.46	0.7068 to 0.8018	0.3272 to 0.37	0.587 to 0.664
Total hydrocarbon production rate, m^3/day-m	-	0.2863 to 0.2068	0.3495 to 0.2410	0.2412 to 0.18	0.2908 to 0.2068	0.2237 to 0.17	0.2625 to 0.1906
Cumulative oil production, m^3/m	153	162.7	165	151.8	150.6	149.3	147
Steam chamber velocity at the top of the reservoir, m/day	0.0368 to 0.0305	0.0395 to 0.0324	0.0403 to 0.0328	0.0366 to 0.0303	0.0364 to 0.03	0.0359 to 0.0298	0.0353 to 0.0292
Maximum distance vapour chamber traveled at the top of the Res., m	32.5	34.63	35.1	32.1	32.1	31.78	31.2
Heat injection rate, J/day-m	6.84E+08	6.81E+08	6.66E+08	6.63E+08	6.44E+08	6.58E+08	6.38E+08
*Additional cum. oil recovery/cum. injected solvent ratio	-	0.29	0.2	-0.038	-0.042	-0.12	-0.11

*Additional oil is defined as cumulative oil by steam plus solvent minus oil by steam only.

Effect of Total Injection Rate

One of the important factors affecting the performance of a solvent-SAGD process is the injection rate. In this section, the performance of a solvent-SAGD process for three different mass injection rates of 300, 400, and 500 kg/ (day-m) are examined. The solvent is butane in all cases at the mass fraction of 9%. A higher total rate of injection at the same mass fraction of the solvent has a higher mass of the solvent plus

steam. For instance, a 500 kg/(day-m) of total injection means 45 kg of the solvent and 455 kg of the steam injection rate per day per unit length of the horizontal well.

Figure 12 compares the oil production rates for these three cases. It is seen that as the total injection rate increases from 300 to 500 kg/ (day-m), the drainage rate increases about 43%. Higher rate of injection reduces bitumen viscosity because of higher temperature and solvent availability in the oil zone and therefore it results in higher oil production rates.

CSORs are compared in Figure 13. Higher injection rate means higher steam injection rate. This means the cumulative steam injection is higher. Higher cumulative oil production is also achieved for a higher injection rate. However, the ratio of these two is greater compared with a lower rate of injection which is undesirable with respect to the process efficiency.

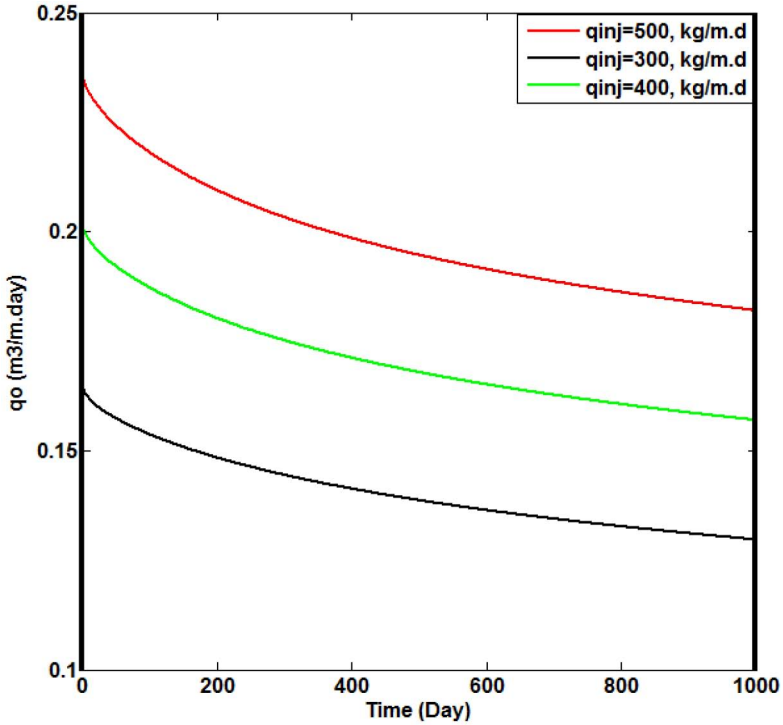

Figure 12—Variation of oil production rate with time for three different total injection rates; 300, 400, and 500 kg/day per unit length of horizontal well.

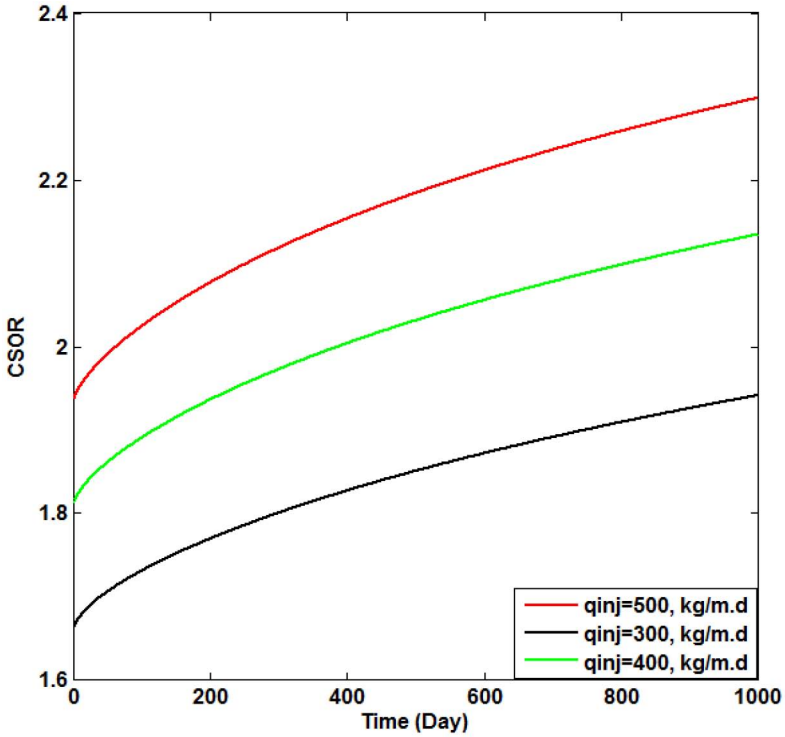

Figure 13—Comparison of CSOR as a function of time for three different total injection rates; 300, 400, and 500 kg/day per unit length of horizontal well.

Figure 14 shows that the solvent loss rate is zero at the beginning of the process and it increases over time. The solvent-SAGD model predicts a higher solvent loss rate for a higher injection rate condition. Higher total rate of the injection also results in higher CSOR.

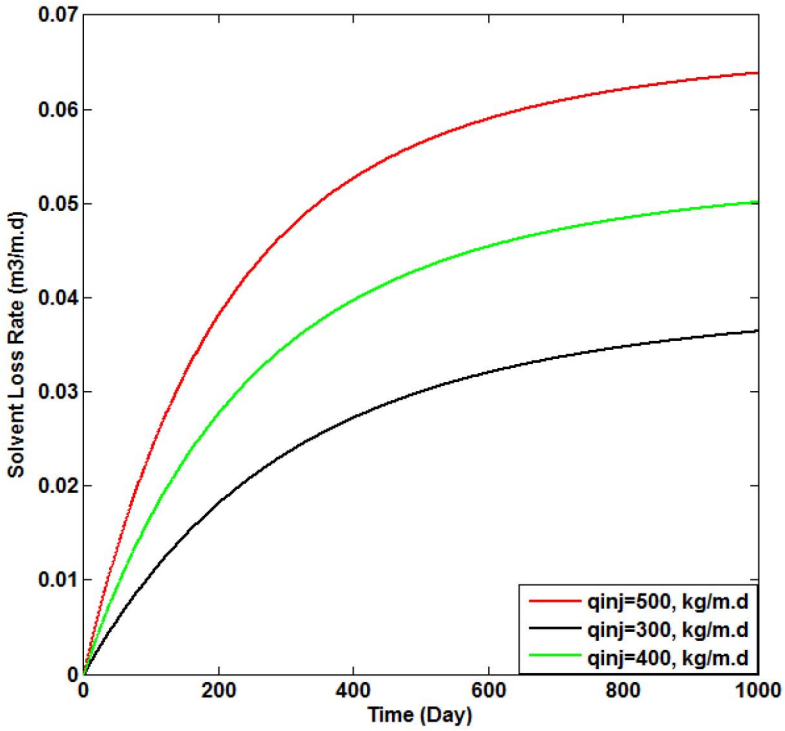

Figure 14—Comparison of solvent loss rate as a function of time for three different total injection rates; 300, 400, and 500 kg/day per unit length of horizontal well.

In conclusion, the new mathematical model of solvent-SAGD process shows that a higher injection rate at the same solvent mass fraction results in a higher oil production but higher CSOR, and Cumulative Solvent-Oil Ratio.

Effect of Solvent Diffusion Coefficient

Solvent diffusion coefficient is a controversial parameter in solvent based recovery. Most of the reported experimental diffusivities of hydrocarbon solvents in heavy oil and bitumen are of the order of $10^{-9}$to 10^{-10} m^2/s (Schmidt, 1989; Upreti and Mehrotra, 2002; Wen and Kantzas, 2005; Afsahi and Kantzas, 2005). In the previous mathematical works in the literature of the solvent-SAGD process, to justify the high oil production rate in a real porous medium, much higher values (almost two orders of magnitude) of the diffusion coefficient than the measured values reported in literature were assumed. Here, the effect of solvent diffusion coefficient is investigated on the performance of the solvent-SAGD process.

The butane diffusion coefficient into the heavy oil used in the base case is 8.04×10^{-4}m^2/day. The diffusion coefficients of one and two orders of magnitude higher than the base case are used for this study. Higher diffusion coefficient means that the solvent at the vapour-oil interface can penetrate further. Figure 15 compares the cumulative oil production for all three cases. The cumulative oil production is higher for a higher diffusivity coefficient.

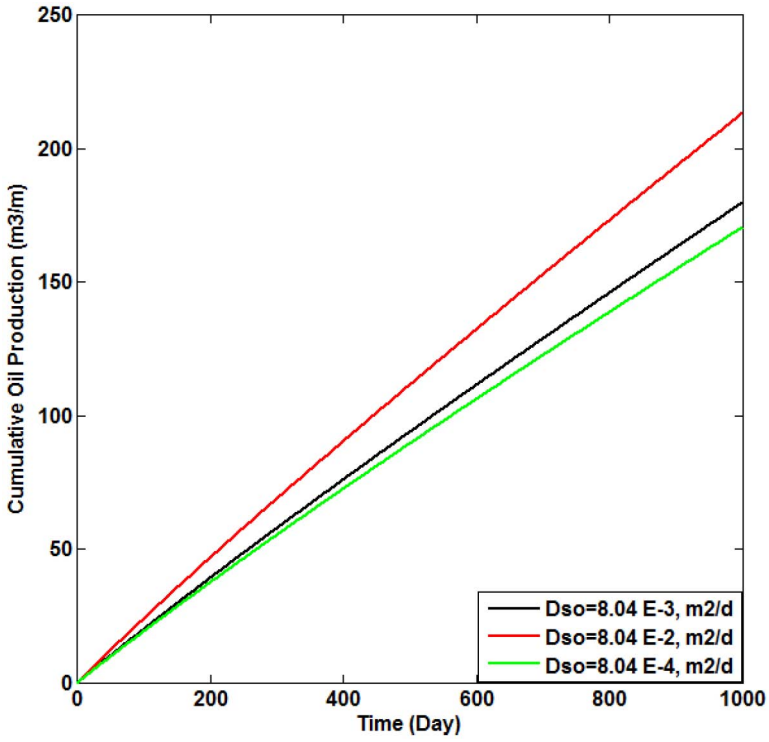

Figure 15—Comparison of cumulative oil production as a function of time for three diffusion coefficients; 8.04×10^{-4}, 8.04×10^{-3}, and 8.04×10^{-2}m^2/day.

Higher diffusivity coefficient at the same rate of injection of the solvent and steam results in lower solvent concentration and temperature due to the limiting effect of constant injection rate, heat and solvent loss. CSOR is lower in the case of a higher solvent diffusivity coefficient as shown in Figure 16. The reason is that in this situation, the cumulative steam injection rate remains unchanged but the cumulative oil production increases.

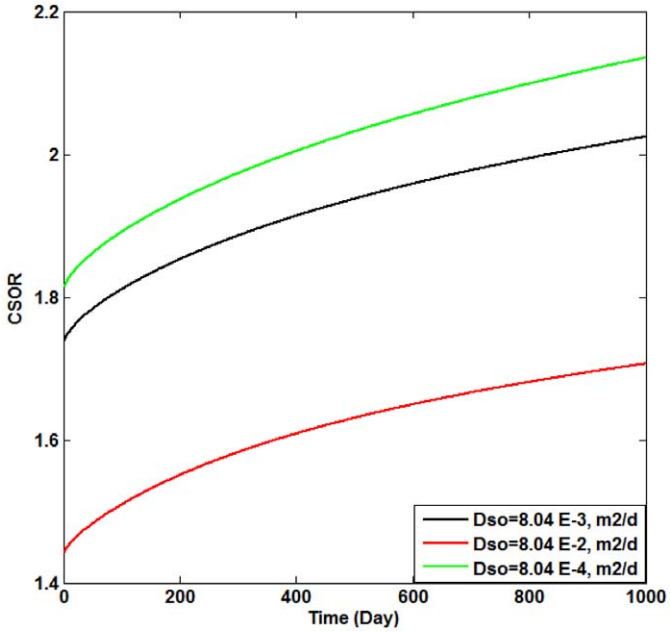

Figure 16—Comparison of CSOR as a function of time for three diffusion coefficients; 8.04×10^{-4}, 8.04×10^{-3}, and 8.04×10^{-2} m^2/day.

Oil Recovery Mechanism

The important factor in analyzing oil production rate in the present approach is how the bitumen viscosity at and close to the interface is affected by different conditions like injection rate, solvent mass fraction, temperature, etc. A higher oil production rate (at the same solvent mass fraction) is achieved by:

1. Increasing injection rate
2. Higher mass diffusion coefficient for solvent-oil

The bitumen viscosity at and close to the interface is different in these two cases. A higher injection rate results in a higher temperature and concentration at the interface but a sharper decrease close to interface. However, a higher diffusion coefficient results in a lower temperature and concentration at the interface compared to the base case but a slower decrease close to the interface.

The solvent-SAGD model is used to analyze the oil recovery mechanism of the base case; butane 9%, solvent diffusion coefficient of $8.04 \times 10^{-4} m^2$/day, and the total mass injection rate of 400 kg/day per unit length of the horizontal well which will be compared with the two cases below:

1. Higher injection rate, Case A; butane 9%, solvent diffusion coefficient of $8.04 \times 10^{-4} m^2$/day, and total mass injection rate of 500 kg/(day — m).
2. Higher diffusion coefficient, Case B; butane 9%, solvent diffusion coefficient of $8.04 \times 10^{2} m^2$/ day, and total mass injection rate of 400 kg/(m — day).

In Case B, the solvent diffusion coefficient is an order of magnitude similar to that of the thermal diffusivity coefficient.

Figure 17 compares the temperature profiles for Case A, and B with the base case. It is clear from the figure that higher and lower temperatures at and close to the interface (distances less than 1 metre) are obtained in Cases A and B compared to the base case, respectively. Considering the effect of heat transfer only, oil viscosity is the lowest in Case A followed by the base case and Case B, respectively.

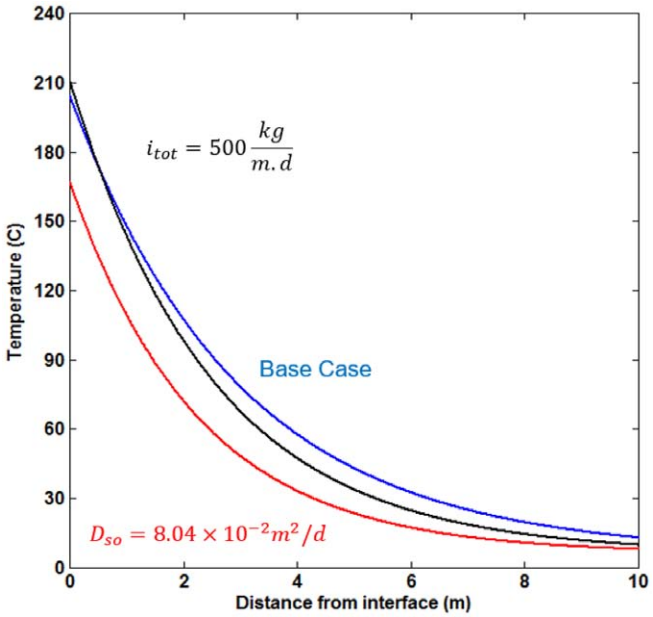

Figure 17—Comparison of temperature profiles for two scenarios with the base case (D_{so} = 8.04 × 10~⁴m²/day, and i_{tot} = 400 *kg/(day — m).);* Case A, higher injection rate, 500 *kg/(day — m)* and Case B, higher diffusion coefficient, 8.04 × *10~²m²/day*.

Figure 18 shows the solvent concentration distribution beyond the chamber edge. The results of the analytical model as seen in this figure, indicate that solvent concentration rises from 18 to 21% as the injection rate is increased (Case A) from 400 to 500 kg/day per unit length of well, but it drops sharply to almost zero at a distance less than 20 cm from the edge. For Case B, the solvent concentration is smaller, just below 10%, at the interface but it decreases gradually as it moves away from the interface.

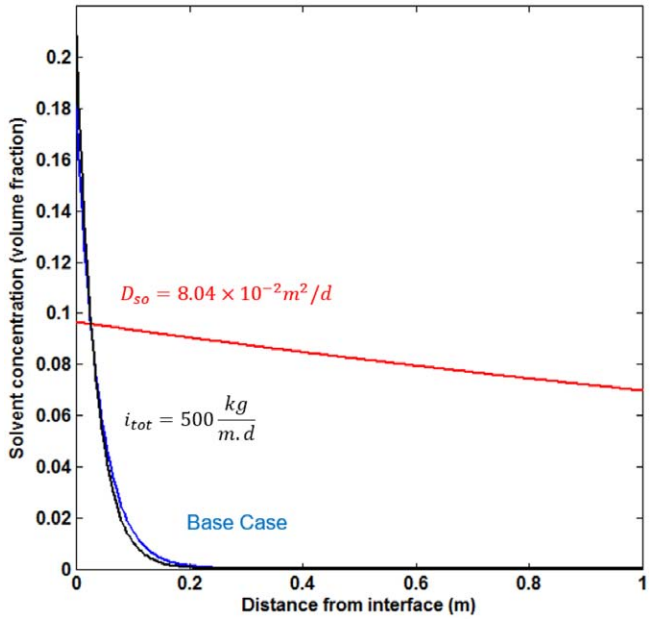

Figure 18—Comparison of solvent concentration profiles for two scenarios with the base case (D_{so} = 8.04 × 10⁻⁴*m²/day*, and i_{tot} = 400 *kg/(day — m).);* Case A, higher injection rate, 500 *kg/(day m)* and Case B, higher diffusion coefficient, 8.04 × *10⁻²m²/day*.

Bitumen viscosity is predicted from the mixture viscosity model introduced in the previous section. It increases with distance from the vapour-oil interface. As a result, the differential drainage rate decreases with distance. Figure 19 shows that bitumen viscosity at a certain distance depends on the temperature

and the solvent concentration at that point. In the case of a higher solvent diffusion coefficient, Case B, bitumen is more viscous at a distance less than 10 cm from the edge compared with the two other cases but the situation appears to reverse afterwards. The oil production rate is proportional to the area under the reciprocal curves of the bitumen viscosity which is a representative of the oil phase mobility ahead of the vapour-oil interface. This area is compared for these three cases in Figure 20. It is seen that the area is greater in Cases A, and B compared with the base case.

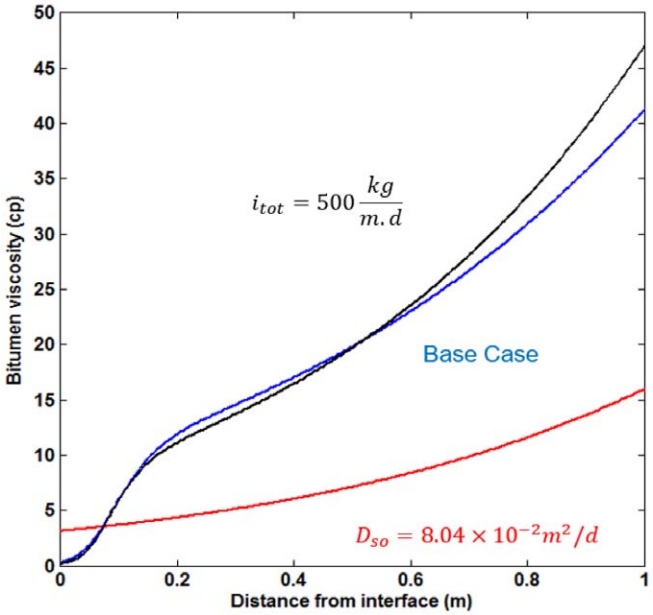

Figure 19—Bitumen viscosity variation for two scenarios with the base case (D_{so} = 8.04 × 10~4m^2/day, and i_{tot} = 400 kg/(day — m).); Case A, higher injection rate, 500 kg/(day — m) and Case B, higher diffusion coefficient, 8.04 × 10~2m^2/day.

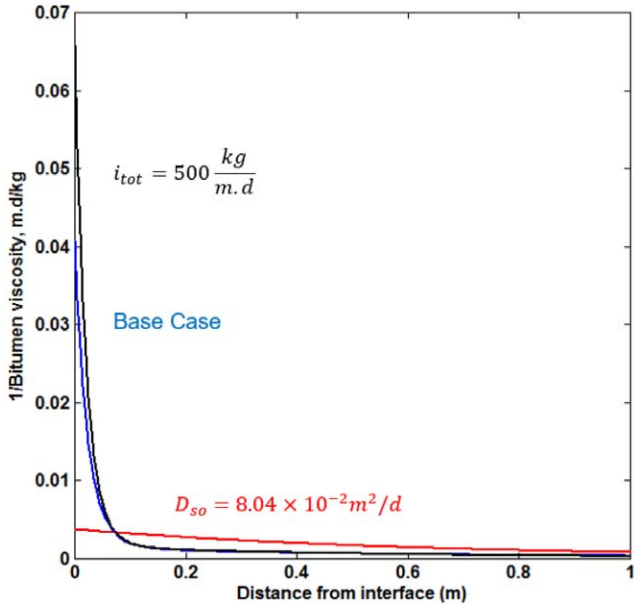

Figure 20—Computed reciprocal of bitumen viscosity as a function of distance from the steam chamber edge.

In a low diffusion coefficient case, the solvent penetration depth is smaller (See Figure 18). Figure 17 shows that the solvent-penetrated zone is at higher temperatures. This results in a lower effect of solvent dilution compared with heating effect on bitumen viscosity reduction. It was shown in the viscosity model

that the significant reduction effect of solvent on bitumen viscosity occurs at lower temperatures. In this situation, heat conduction largely controls the bitumen drainage rate.

In this approach, a higher solvent diffusion coefficient results in lower temperature and solvent concentration values but at a larger distance from the chamber edge (See Figure 17 and 18). Oil recovery mechanism in this situation is mostly controlled by solvent dilution effect on bitumen. The reason is that a lower temperature means a higher bitumen viscosity. However, this negative effect is offset by the positive effect of the bitumen dilution on viscosity reduction. Therefore, the model results indicate that at a larger assumed diffusion coefficient, the system is forced to be controlled by mass transfer at lower temperatures instead of heat transfer.

It is important to note that a higher diffusion coefficient, $8.04 \times 10{\sim}^{2} m^2/day$, results in unrealistic mass diffusion penetration depth changing from several centimetres to several metres (See Figure 18). By increasing the injection rate, the oil production rate is dominantly controlled by bitumen viscosity reduction due to the heating effect.

Conclusion

1. Mass transfer occurs over a scale of centimetres, while heat transfer scale is of the order of metres.
2. It is concluded that the solvent-SAGD process would yield a higher oil recovery, if viscosity reduction from dilution at a lower temperature is greater than viscosity reduction by temperature in the plain SAGD process, for the same total injection rate. For example, 9% wt butane added to steam led to a higher oil recovery than 5% wt butane, or steam alone, while pentane and hexane did not, for the same conditions, resulting in the lowest CSOR for butane. An increase in the mass fraction of butane yielded higher recovery, whereas the heavier hydrocarbons had the opposite effect.
3. An important number is the ***additional*** cumulative oil to injected solvent ratio, which was found to be positive for butane only; the number was much lower than 1 which indicates that the gain in bitumen volume produced was lower than the volume of butane injected.
4. It is shown that the total injection rate (steam plus solvent) leads to a higher recovery, because both the temperature and solvent concentration at the interface are generally higher than for a lower rate. However, CSOR and Cumulative Solvent-to-Oil Ratio, as well as solvent retention increase with rate.
5. It is concluded that the solvent diffusion coefficient has a complex effect on performance. A large diffusion coefficient leads to higher oil production, as the depth of penetration is greater than for a lower coefficient, and bitumen dilution is the controlling factor. For a low diffusion coefficient (the real case), depth of penetration is small but the temperature is higher and viscosity reduction by heat is the controlling factor.
6. This study indicates that although the mixture of bitumen and solvents results in lower viscosity compared with bitumen only over the entire range of temperatures, this does not mean in a solvent-SAGD process which is a combination of heat and mass transfer, always a higher oil production should be expected.

Nomenclature

A_{inf}	Steam/oil Interface area per unit length of horizontal well, m^2/m
C	Heat capacity, J/kg. °C
C	Solvent volume fraction in solvent-bitumen mixture
C_{sol}^{inj}	Injected solvent mass fraction
D_{so}	Diffusion coefficient of solvent in bitumen, m^2/day
H	Reservoir thickness, m
K_{ob}	Overburden thermal conductivity, J/m.day.°C

K_{res} Reservoir thermal conductivity, J/m.day.°C
k_{abs} Absolute permeability, m²
k_o Effective oil permeability, m²
L_v Latent heat of condensation, J/kg
q_{inj} Rate of heat injection, J/m.day
$qioss$ Rate of heat loss, J/m.day
q_0 Oil production rate, m³/m.day
q_{res} Heat rate into the reservoir, J/day.m
S_{oi} Reservoir initial oil saturation, fraction
S_{or} Residual oil saturation in steam chamber, fraction
t Time, day
T Temperature, °C
T_D Dimensionless temperature
T_r Reservoir temperature, °C
T_s Steam temperature, °C
U_f Heat front velocity, m/day
x'_H Steam chamber velocity at the top of the reservoir, m/day
x'_y Steam chamber velocity at special y, m/day
α Reservoir thermal diffusivity, m²/day
α_{ob} Overburden thermal diffusivity, m²/day
θ Angle of steam/oil interface to the horizon
μ_o Dynamic oil viscosity, kg/m.day
ξ Coordinate perpendicular to steam/oil interface, m
ρ_o Oil density, kg/m³
φ Porosity, fraction

References

Afsahi, B., and Kantzas, A. 2005. Effect of the presence of sand on solvent diffusion in bitumen. Presented at the Canadian International Petroleum Conference, Calgary, Alberta, 7-9 June. PETSOC-2005- 092. https://doi.org/10.2118/2005-092.

Andrade, E.C. 1930. The viscosity of liquids. *Nature* **125** (3148): 309–310. https://doi.org/10.1038/125582a0.

Azom, P.N., and Srinivasan, S. 2013. Modeling Coupled Heat Transfer and Multiphase Flow during the Expanding Solvent Steam-Assisted Gravity Drainage (ES-SAGD) Process. Presented at the SPE Annual Technical Conference and Exhibition, New Orleans, Louisiana, USA 30 September-2 October. SPE-166357-MS. https://doi.org/10.2118/166357-MS.

Butler, R., and Mokrys, I. 1989. *Solvent Analog Model of Steam-Assisted Gravity Drainage*, Vol. **05**.p.17, AOSTRA Journal of Research (Reprint).

Das, S.K., and Butler, R.M. 1998. Mechanism of the vapor extraction process for heavy oil and bitumen. *Journal of Petroleum Science and Engineering* **21** (1): 43–59. https://doi.org/10.1016/S0920-4105(98)00002-3.

Farouq Ali, S., and Abad, B. 1976. Bitumen recovery from oil sands, using solvents in conjunction with steam. *Journal of Canadian Petroleum Technology* **15** (03). PETSOC-76-03-11. https://doi.org/10.2118/76-03-11.

Gupta, S.C., and Gittins, S. 2011. A Semi-analytical Approach for Estimating Optimal Solvent Use in a Solvent Aided SAGD Process. Presented at the SPE Annual Technical Conference and Exhibition, Denver, Colorado, USA, 30 October-2 November. SPE-146671-MS. https://doi.org/10.2118/146671-MS.

Nasr, T.N., and Isaacs, E.E. 2001. *Process for enhancing hydrocarbon mobility using a steam additive*, US Patent No. 6230814 B1, 15 May (Reprint).

Rabiei Faradonbeh, M., Harding, T.G., and Abedi, J. 2014. Semi-Analytical Modeling of Steam-Solvent Gravity Drainage of Heavy Oil and Bitumen, Part 2: Unsteady-State Model With Curved Interface. Presented at the SPE Heavy Oil Conference-Canada, Calgary, Alberta, Canada 10-12 June. SPE- 170123-MS. https://doi.org/10.2118/170123-MS.

Schmidt, T. 1989. Mass transfer by diffusion. *AOSTRA Handbook on Oil Sands, Bitumens and Heavy Oils.*

Shu, W. 1984. A viscosity correlation for mixtures of heavy oil, bitumen, and petroleum fractions. *Society of Petroleum Engineers Journal* **24** (03): 277–282. SPE-11280-PA. https://doi.org/10.2118/11280-PA.

Upreti, S.R., and Mehrotra, A.K. 2002. Diffusivity of CO2, CH4, C2H6 and N2 in Athabasca bitumen. *The Canadian Journal of Chemical Engineering* **80** (1): 116–125. https://doi.org/10.1002/cjce.5450800112.

Vogel, J. 1984. Simplified heat calculations for steamfloods. *Journal of petroleum technology* **36** (07): 1,127–1,136. SPE-11219-PA. https://doi.org/10.2118/11219-PA.

Wen, Y., and Kantzas, A. 2005. Monitoring bitumen- solvent interactions with low-field nuclear magnetic resonance and X-ray computer-assisted tomography. *Energy & fuels* **19** (4): 1319–1326. https://doi.org/10.1021/ef049764g.

Zargar, Z., and Farouq Ali, S.M. 2017. Analytical Treatment of Steam-Assisted Gravity Drainage: Old and New. *Society of Petroleum Engineers Journal.* SPE-180748-PA. 10.2118/180748-PA.